J. Min. Metall. Sect. B-Metall. 53 (3) B (2017) 413 - 422

Journal of Mining and Metallurgy, Section B: Metallurgy

PHASE TRANSFORMATION AND MICROSTRUCTURE STUDY OF THE AS-CAST Cu-RICH Cu-Al-Mn TERNARY ALLOYS

T. Holjevac Grgurić [a,*], D. Manasijević [b], S. Kožuh [a], I. Ivanić [a], Lj. Balanović [b], I. Anžel [c], B. Kosec [d], M. Bizjak [d], M. Knežević [a], M. Gojić [a]

[a] Faculty of Metallurgy, University of Zagreb, Sisak, Croatia
[b] University of Belgrade, Technical Faculty Bor, Bor, Serbia
[c] Faculty of Mechanical Engineering, University of Maribor, Maribor, Slovenia
[d] Faculty of Natural Sciences and Engineering, University of Ljubljana, Ljubljana, Slovenia

(Received 09 August 2017; accepted 19 September 2017)

Abstract

Four Cu-rich alloys from the ternary Cu-Al-Mn system were prepared in the electric-arc furnace and casted in cylindrical moulds with dimensions: ϕ=8 mm and length 12 mm. Microstructural investigations of the prepared samples were performed by using optical microscopy (OM) and scanning electron microscopy, equipped by energy dispersive spectroscopy (SEM-EDS). Assignation of crystalline phases was confirmed by XRD analysis. Phase transition temperatures were determined using simultaneous thermal analyzer STA DSC/TG. Phase equilibria calculation of the ternary Cu-Al-Mn system was performed using optimized thermodynamic parameters from literature. Microstructure and phase transitions of the prepared as-cast alloys were investigated and experimental results were compared with the results of thermodynamic calculations.

Keywords: Cu-Al-Mn alloys; SMA alloys; Microstructure; Phase transformations.

1. Introduction

The trigger for wide research of Cu-Al-Mn alloys in recent years is their easy manufacturing, low cost as well as good properties, especially electric properties and thermal conductivity. The special emphasis of investigations are Cu-Al-Mn shape memory alloys (SMA), that shows unique properties of remembering their shape as well as recovering to original shape under temperature changes or plastic deformation [1-4]. Cu-Al-Mn alloys display advantage in technological applications over other Cu-based SMA alloys, such as Cu-Al-Ni, Cu-Al-Zn etc., according to significantly higher ductility and ability of cold deformation [5,6]. The addition of quaternary element to Cu-Al-Mn alloys, improves their properties and meet the standards for application as sensors or actuators, in automotive industry, robotics, aerospace or biomedical sectors [7-9]. Sutou and co-authors investigated the influence of Ti, Cr, Co, Fe, Ag, Au, Ni, Zn, Si and Sn on the shape memory effect and pseudoelasticity of Cu-Al-Mn alloys [10]. He reported that addition of Fe, Au, Zn, Ni and Ti improves shape memory effect (SM) of alloys, while Co, Si, Sn and Cr decrease temperature of martensitic transformation (M_s) as well as their ability to cold-workability. The effect of Ce on the microstructure and phase transformation temperatures on Cu-Al-Mn SMA alloy was reported by Chen [11], while Canbay presented the effect of Fe on the enthalpy and entropy values of Cu-Al-Mn-Fe system [12].

From thermodynamic point of view, binary systems Cu-Al, Cu-Mn and Al-Mn are well known, but ternary Cu-Al-Mn system is still the object of intensive investigations [13-17]. Cu-Al system was studied extensively by Murray and Liu [14, 18, 19]. Thermodynamic description of Cu-Mn binary system was given Cuiyun He, Young Du and co-authors [20] and Mn-Al system by Young Du and A. Shukla [21, 22].

Single β-phase in Cu-Al binary system is stable in compositions of 20 – 28 % of aluminium, but the addition of manganese stabilizes β-phase and widens the composition region. β-phase is parent phase for formation of martensitic β` phase, and consequently causes shape memory (SM) and pseudoelasticity (PE)

Dedicated to the memory of Professor Dragana Živković

* *Corresponding author: tholjev@simet.hr*

DOI:10.2298/JMMB170809039H

effects in material [23]. In wide composition range of β-phase, in Cu-Al-Mn alloys, order-disorder transitions occur: A2 (disordered bcc Cu) – B2 (CuAl) – $L2_1$ (Cu_2AlMn). Heusler, $L2_1$, phase has ferromagnetic properties, as a result of atomic ordering of manganese atoms [19]. Kainuma [24] reported that low aluminium content, lower than 17 % at. shows excellent ductility of Cu-Al-Mn alloys as well as cold-workability, due to lower degree of order of β-parent phase. Vis-a-vis, SM properties decrease with aluminium content and with A2 parent phase [25]. Therefore, the balanced composition of Al and Mn elements in ternary alloy is crucial for its final properties. Thermodynamic description of the ternary Cu-Al-Mn system was given by Lucas [26] and Miettinen [27]. Miettinen gave parameters optimized according to experimental procedure for ternary system, but only for Cu-rich corner of phase diagram.

In this paper, the influence of different contents of aluminium and manganese in Cu-rich ternary Cu-Al-Mn alloys on the thermodynamic equilibrium, microstructure and phase transformation temperatures is reported.

2. Experimental

Cu-Al-Mn alloys were prepared by melting of raw materials from manufacturer MaTeck Material-Technologie&Kristalle GmbH: copper, purity of 99.99 % (pellets 6x6 mm), aluminium, purity of 99.99 % (granules 2-10 mm) and manganese, purity of 99.99 % (pieces 3-12 mm). Melting of pure metals was performed in the electric-arc furnace, under argon atmosphere. Samples were re-melted 3 times due to better homogenization of alloy, with cycles of vacuuming and 15 minutes argon leakaging before each re-melting. After that, samples were casted in the cylindrical moulds with dimensions: diameter of 8 mm and length of 12 mm. Experimentally determined samples compositions based on results of EDS analysis are given in Table 1.

Table 1. *Chemical composition of investigated Cu-Al-Mn alloys*

	Chemical composition		
Sample	(% wt.)		
	Cu	Al	Mn
1	85.1	5.5	9.4
2	83.3	7.1	9.6
3	89.9	1.2	8.9
4	78.5	11.4	10.1
Standard uncertainties (EDS mesurement)	±2-2.3 %	±0.1-0.5 %	±0.3-0.4%

Samples were prepared for microstructural investigations by inserting into the conductive paste by Automatic Mounting Press Buehler SimpliMet 1000. Grinding was performed by Buehler machine, with water-cooled SiC papers from 240 till 1200 grit, at force of 5 N and speed 150 rpm/min. Polishing was done by microfiber felt with diluted alumina solution, at same force and speed.

Prepared specimens were etched with solution of 2,5 g $FeCl_3$/48 mL CH_3OH/10mL H_20.

Microstructure of Cu-Al-Mn shape memory alloys was determined by Optical Microscope Olympus GX 51, with image analysis software, Analysis Materials Research Lab., Japan, as well as with Scanning Electron Microscope Tescan Vega, equipped by Energy Dispersive Spectroscopy (EDS), Brücher. The microscope was operated by Secondary electron detector, at acceleration voltage of 20 kV. Calibration for the quantitative measurements was performed by Au standard. XRD analysis was performed by PANalytical, X'Pert PRO, $CuKa_1$ radiation, from 15 to 90°, with rate of 2°/min. Transformation temperatures were obtained by Simultaneous Thermal Analysis, Differential Scanning Calorimetry / Thermogravimetry, with instrument STA DSC/TG, NETZSCH Jupiter 449 F1. Temperature and sensitivity calibration files were created with measurements of 8 different pure materials: In, Sn, Bi, Pb, Zn, Al, Ag and Ni. The resolution of DSC instrument was < 1μm and temperature resolution 0.001 K. Dynamic measurements were performed in the temperature interval from 25 °C to 1150 °C, in argon atmosphere, with heating/cooling rate of 10 °C/min. Thermodynamic calculations of phase diagram were done by PANDAT software.

3. Thermodynamic calculations

Thermodynamic calculations performed in this work are based on the CALPHAD method and minimization of Gibbs free energy of system [28, 29]. In this work calculation were done using thermodynamic parameters of pure elements according to SGTE database [30] and optimized thermodynamic parameters from Miettinen [27]. Phases considered in calculation with their crystallographic data are presented in Table 2.

4. Results and Discussion

Fig. 1 shows calculated part of the vertical section of the Cu-Al-Mn ternary system with constant Mn content (9.4 %wt. Mn) and with labeled composition of the investigated Cu-5.5 %wt. Al-9.4 %wt. Mn alloy and calculated diagram of the phase fractions at different temperatures under equilibrium conditions.

From Fig. 1 it could be seen that during cooling of

Table 2. *Crystalographic data for the considered phases in ternary Cu-Al-Mn system [26]*

Phase / Temperature range	TD database name	Pearson symbol	Space group	Lattice Parameters [pm]
Liquid	L	-	-	-
fcc (Cu)	FCC_A1	*cF4*	*Fm3m*	*a* = 361.48
< 1083				
β	BCC_ A2	*cI2*	*Im3m*	*a* = 294.6
1049-761				
γ	GAMMA	*cF4*	*P43m*	*a* = 871.32
< 873				
cbcc (αMn)	CBCC_A12	*cI58*	*I43m*	*a* = 891.39
< 710				
τ_3	Cu_3Mn_2Al	*cF24*	*Fd3m*	*a* = 690.46
< 550				

the Cu-5.5 %wt. Al-9.4 %wt. Mn alloy under equilibrium conditions, α-phase (fcc Cu) starts to solidify at 973 °C. β-phase (bcc Cu) is stable in the narrow temperature interval from 923 till 899 °C. Solidus temperature is determined at 920 °C, while low temperature ternary phase Cu_3Mn_2Al, known as τ_3-phase, precipitates at 435 °C from the α-phase and stay stable till room temperature jointly with α-phase.

Microstructural analysis of Cu-5.5 %wt. Al-9.4 %wt. Mn alloy shows two-phase morphology, where according to EDS based compositions matrix is identified as α-phase, while the composition of the discrete phase fit well to that of Cu_3Mn_2Al (τ_3) phase (Fig. 2 and 3). Experimental results are in agreement with the results of phase equilibria calculation.

Transformation temperatures obtained under non-equilibrated heating of specimen from room temperature till 1150 °C in the DSC cell are given in Fig. 4. Small endotherm detected at 405 °C is described as beginning of dissolution of Cu_3Mn_2Al (τ_3) phase, while the second peak, observed at 765 °C to dissolution of β-phase. Solidus temperature is determined at 915°C, which is in very good agreement with thermodynamic calculations shown in Fig. 1 (T_s = 920 °C).

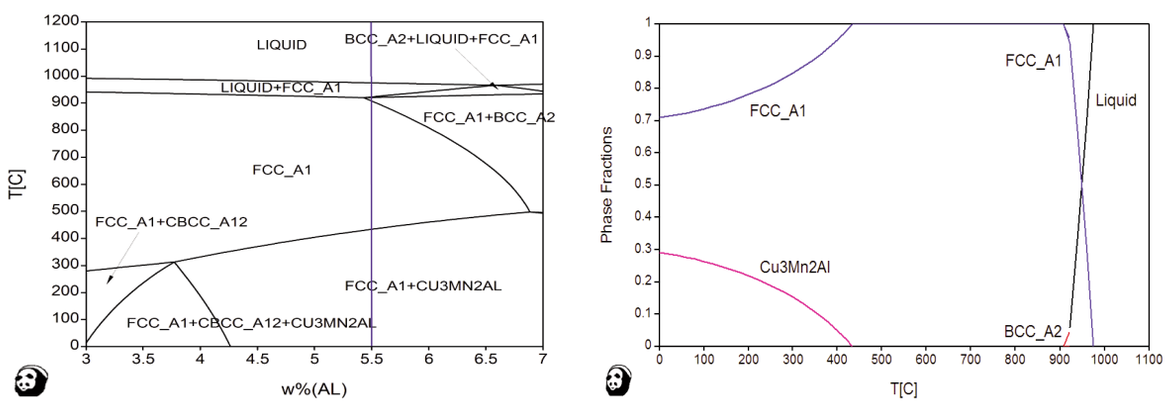

Figure 1. *Thermodynamic calculations for the Cu-5.5 %wt. Al-9.4 %wt. Mn alloy a) part of the calculated vertical section of the Cu-Al-Mn ternary system with constant Mn content (9.4 %wt. Mn) and with marked composition of the investigated alloy b) calculated phase fractions with temperature in equilibrium condition for the investigated alloy*

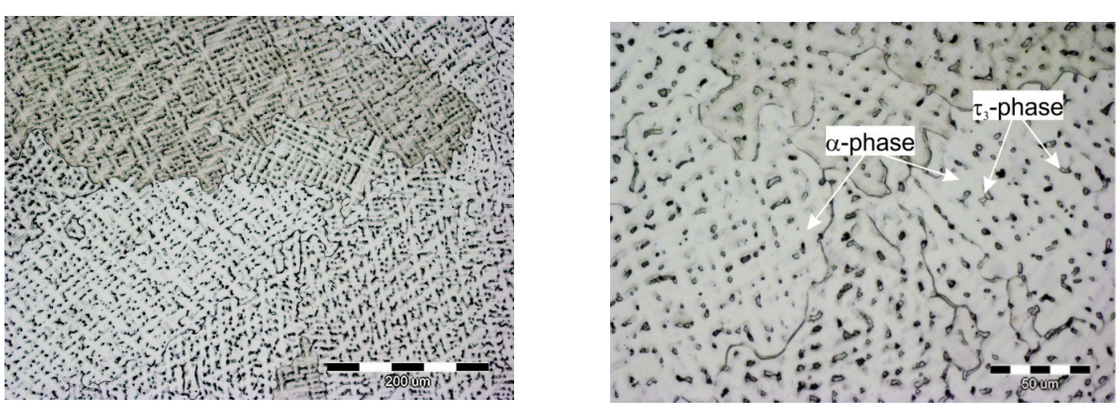

Figure 2. *OM micrographs of Cu-5.5 %wt. Al-9.4 %wt. Mn alloy at magnification: a) 200 x, b) 500 x*

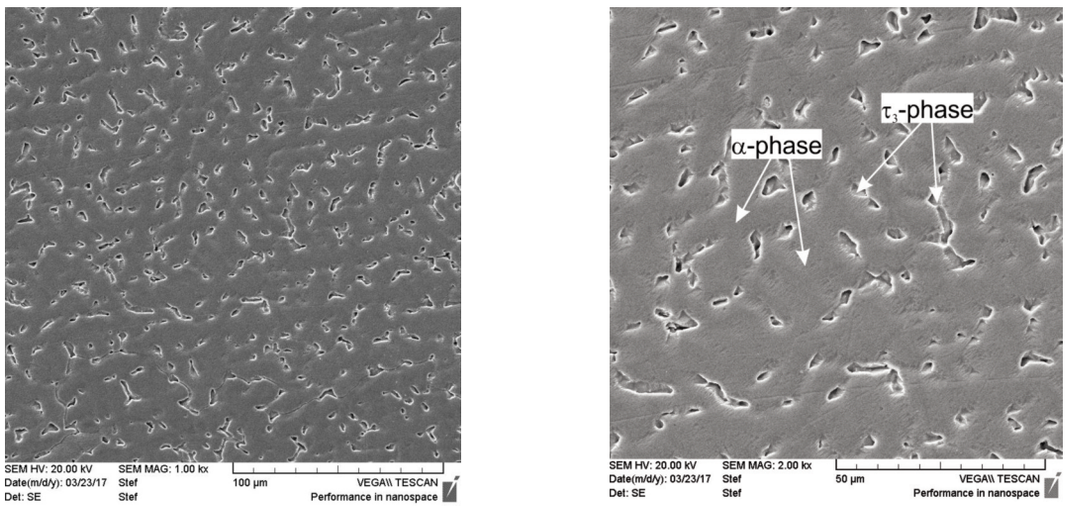

Figure 3. *SEM micrographs of Cu-5.5 %wt. Al-9.4 %wt. Mn alloy at magnification: a) 1000 x, b) 2000 x*

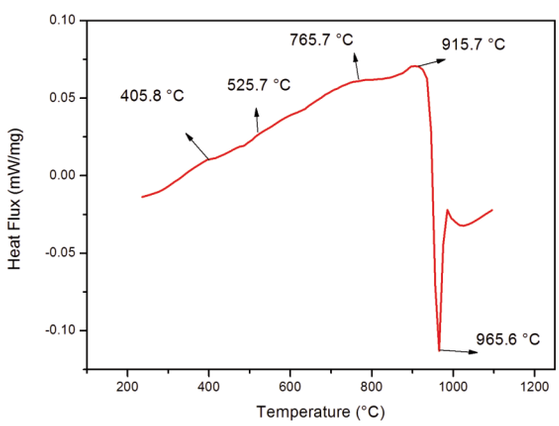

Figure 4. *DSC heating curve for sample Cu-5.5 %wt. Al-9.4 %wt. Mn*

According to thermodynamic calculations expected stable phases for the Cu-7.1%wt. Al-9.6%wt. Mn alloy at room temperature are α-phase (Cu fcc phase) and τ_3 (Cu_3Mn_2Al phase) (Fig. 5a,5b). The results of microstructural analysis for the Cu-7.1%wt. Al-9.6%wt. Mn alloy pointed out the two-phase α+β morphology, as can be seen from OM and SEM micrographs in Figs 6 and 7. XRD analysis in Bragg-Brentano setup was employed to support the microscopy findings. The samples where SEM was not conclusive (Cu-7.1 %wt. Al-9.6 %wt. Mn and Cu-1.2 %wt. Al- 8.9 %wt. Mn) were selected in order to reveal more from their diffraction patterns. Both samples exhibit only few diffraction lines, some of them with very high intensities. XRD analysis of the Cu-7.1%wt. Al-9.6%wt. Mn alloy confirms dominant α-phase (Cu fcc phase), with the presence of β-phase, with ordered

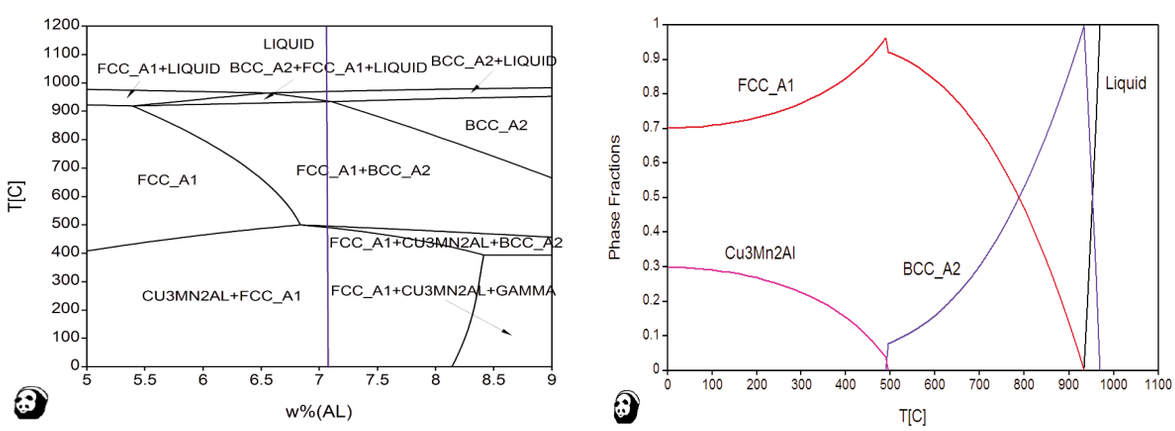

Figure 5. *Thermodynamic calculations for the investigated Cu-7.1 %wt. Al-9.6 %wt. Mn alloy a) part of the calculated vertical section of the Cu-Al-Mn ternary system with constant Mn content (9.6 %wt. Mn) and with marked composition of the investigated alloy, b) calculated phase fractions with temperature in equilibrium condition for the investigated alloy*

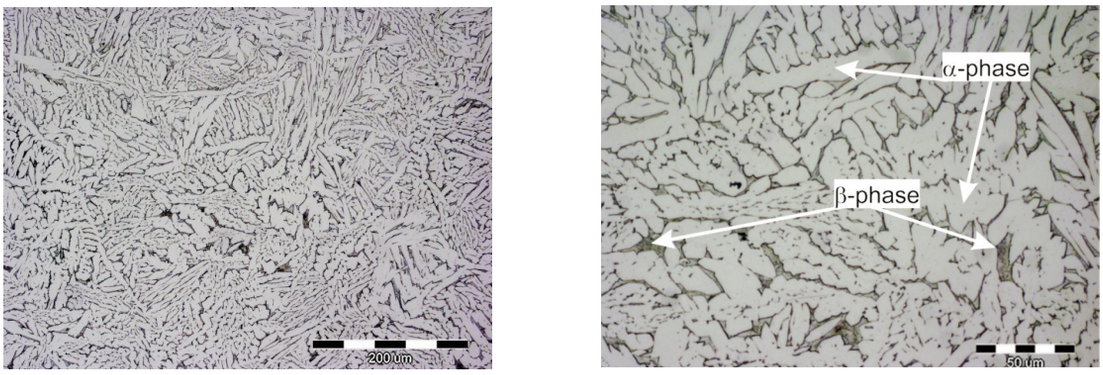

Figure 6. *OM micrographs of sample Cu-7.1 %wt. Al-9.6 %wt. Mn at magnification: a) 200 x, b) 500 x*

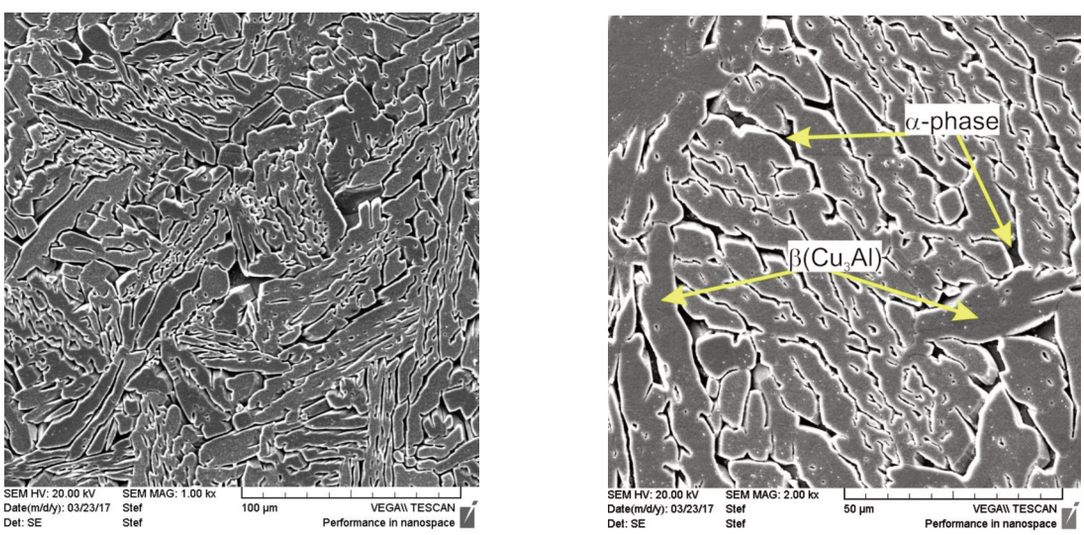

Figure 7. *SEM micrographs of sample Cu-7.1 %wt. Al-9.6 %wt. Mn at magnification:* a) 1000 x, b) 2000 x

DO_3 (Cu_3Al) phase (Fig 8). According XRD results, τ_3-phase is present in this sample only in traces.

During cooling β-phase undergoes to order-disorder transitions, as mentioned earlier, from A2 – B2 – DO_3 (Cu_3Al) or $L2_1$ (Cu_2AlMn).

Thermodynamic description wasn't included

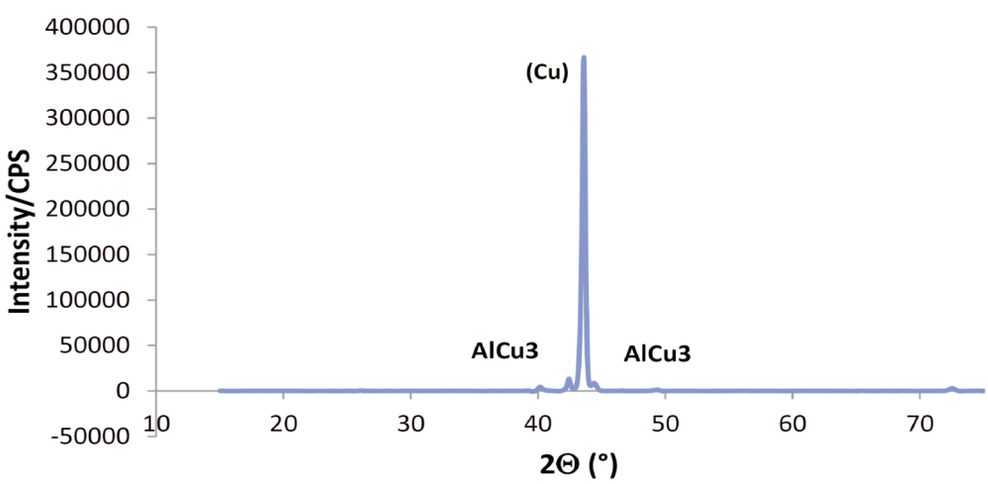

Figure 8. *XRD diffractogram for the Cu-7.1 %wt. Al-9.6 %wt. Mn*

ordering transformations because of lack of optimized thermodynamic data. According to the previous investigations [24], both ordering transitions depend on the content of aluminium rather than content of manganese in alloy. Decreased amount of aluminium in ternary alloy affects precipitation of α-Mn (cbcc-phase) as it is predicted by the results of thermodynamic calculations shown in Fig 9. During cooling of Cu-1.2 %wt. Al-8.9 %wt. Mn alloy, α-Mn (cbcc phase) starts to precipitate at 174 °C (Fig. 9). Precipitation of α-Mn is obvious from optical and SEM micrographs (Figs 10 and 11) and it is confirmed by X-ray diffraction (Fig 12).

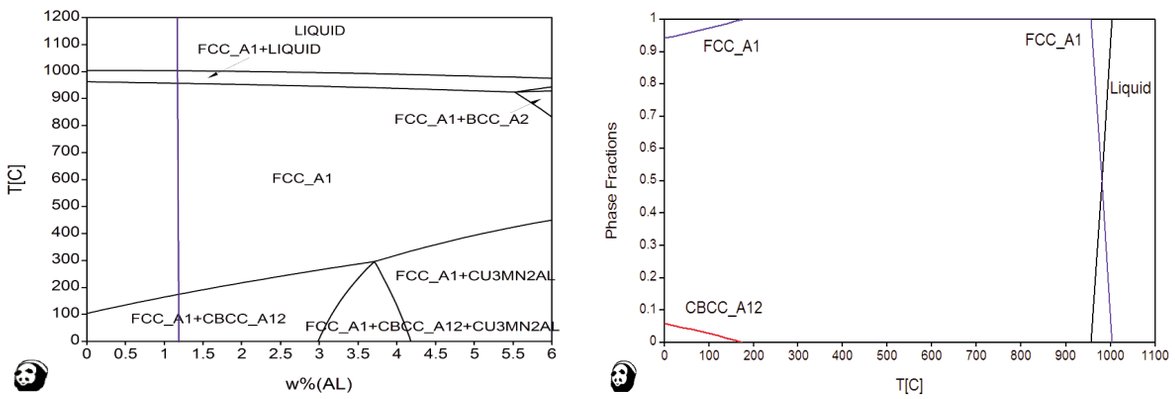

Figure 9. *Thermodynamic calculations for the investigated Cu-1.2 %wt. Al-8.9 %wt. Mn alloy: b) part of the calculated vertical section of the Cu-Al-Mn ternary system with constant Mn content (8.9 %wt. Mn) and with marked composition of the investigated alloy, b) calculated phase fractions with temperature in equilibrium condition for the investigated alloy*

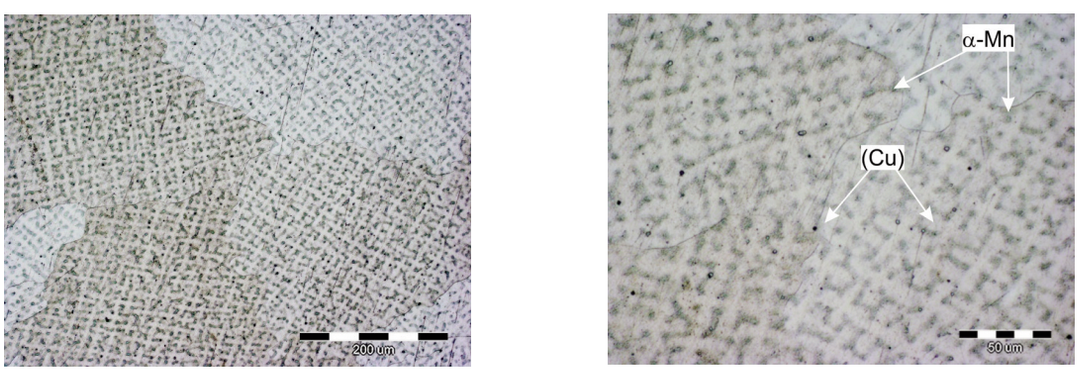

Figure 10. *OM micrographs of Cu-1.2 %wt. Al- 8.9 %wt. Mn at magnification: a) 200 x,b) 500 x*

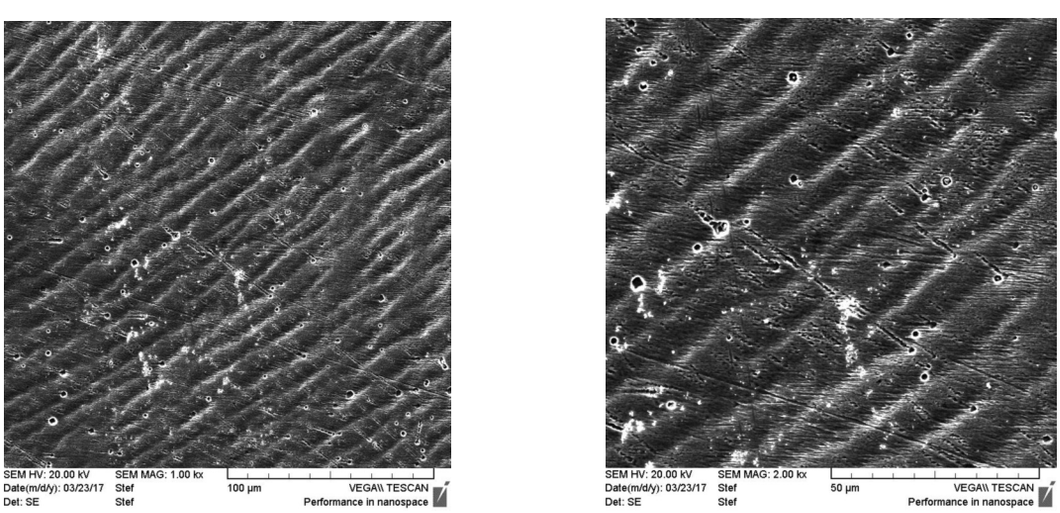

Figure 11. *SEM micrographs for sample Cu-1.2 %wt. Al- 8.9 %wt. Mn at magnification: a) 1000 x, b) 2000 x*

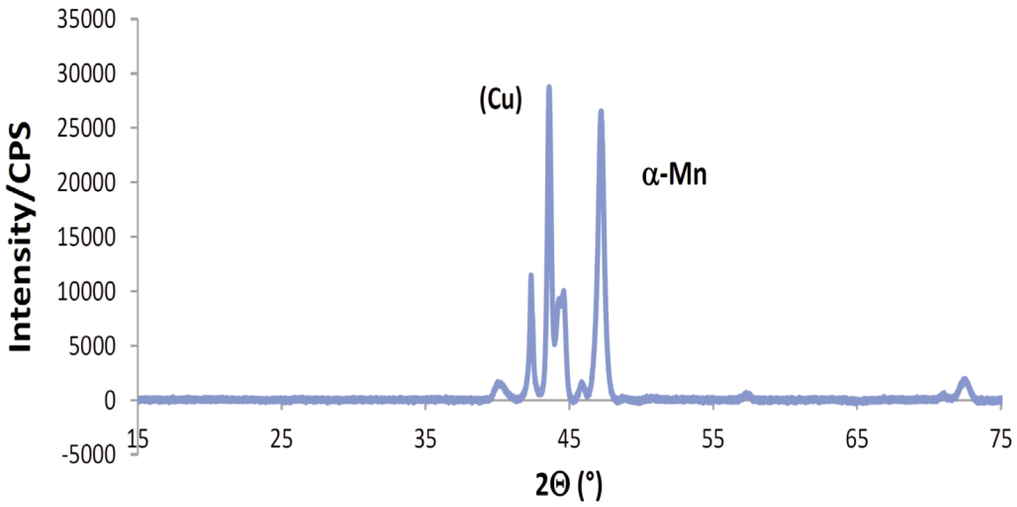

Figure 12. *X-ray diffraction pattern for the Cu-1.2 %wt. Al- 8.9 %wt. Mn alloy*

Position of related DSC peak is observed at 194 °C (Fig 13). It should be noted that solidus temperature as well as onset temperature for melting of α-phase are somewhat lower than theoretical values, T_s = 943 °C and T_a = 975 °C (Fig 13).

Cu-11.4%wt. Al- 10.1%wt. Mn alloy solidifies with primary cristalization of β-phase (bcc phase) and at 393 °C ternary eutectoid reaction $\alpha + \gamma + \tau_3 \leftrightarrow \beta$ occurs, with formation of τ_3-phase (Cu_3Mn_2Al) (Fig 14a, 14b). Optical and SEM images of the microstructure are presented in Figs 15 and 16.

DSC results show dissolution of τ_3 phase at 500 °C and α and γ phases at lower temperature, around 300 °C (Fig 17). Endothermic peak detected around 700 °C probably is related to order-disorder transition B2/A2.

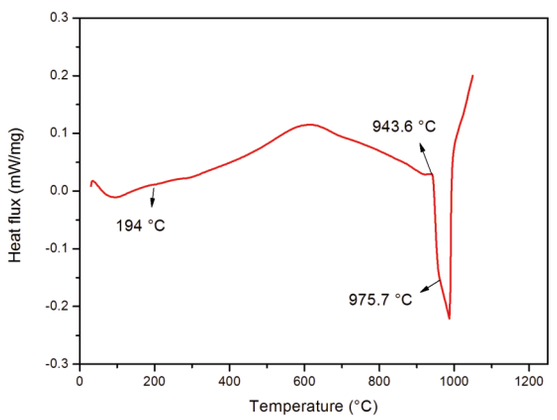

Figure 13. *DSC heating curve of Cu-1.2 %wt. Al-8.9 %wt. Mn alloy*

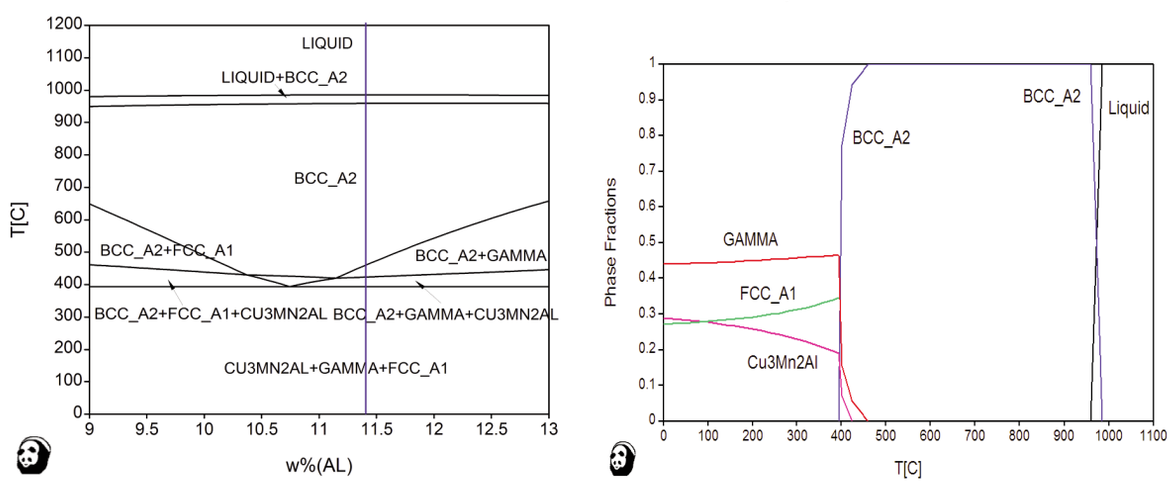

Figure 14. *Thermodynamic calculations for the investigated Cu-11.4%wt. Al- 10.1%wt. Mn alloy: a) part of the calculated vertical section of the Cu-Al-Mn ternary system with constant Mn content (10.1 %wt. Mn) and with marked composition of the investigated alloy, b) calculated phase fractions with temperature in equilibrium condition for the investigated alloy*

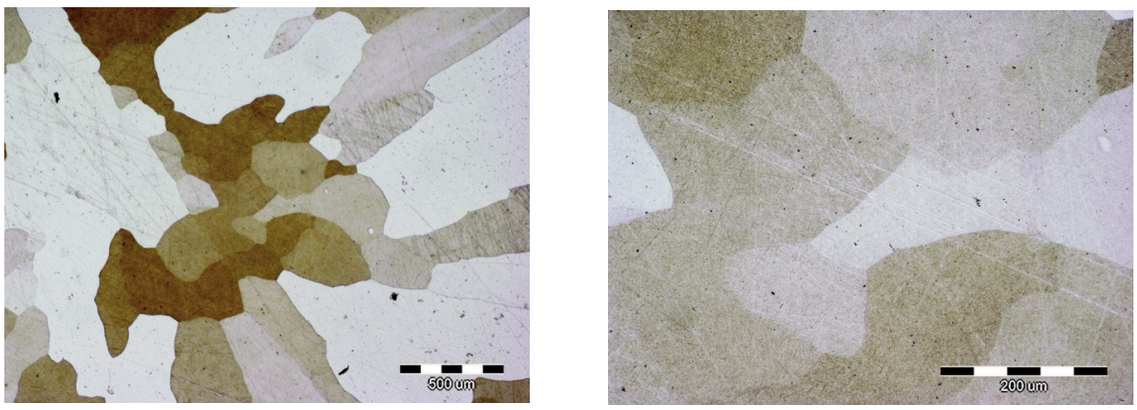

Figure 15. *OM micrographs of Cu-11.4%wt. Al- 10.1%wt. Mn alloy at magnification: a) 50 x, b) 200 x*

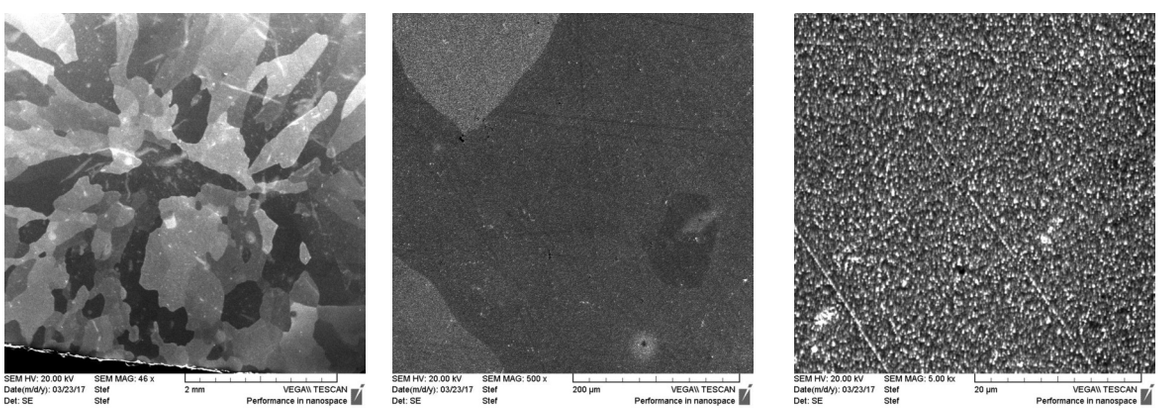

Figure 16. *SEM micrographs of Cu-11.4%wt. Al- 10.1%wt. Mn alloy at magnification: a) 46 x, b) 500 x, c) 5000 x*

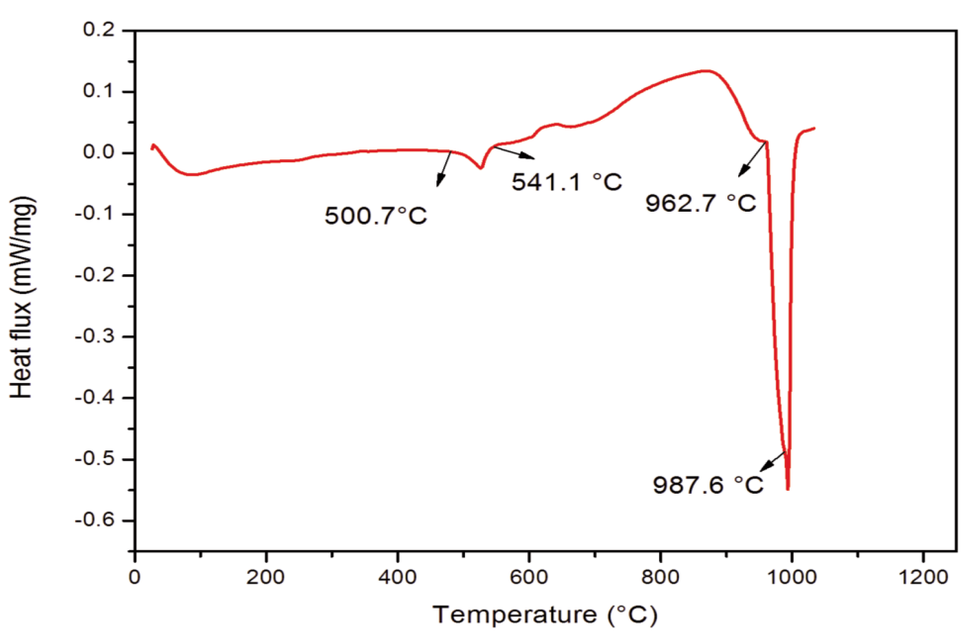

Figure 17. *DSC analysis of Cu-11.4%wt. Al- 10.1%wt. Mn alloy*

Solidus temperature is determined at 962 °C, and melting of β-phase at 987 °C. Similar composition of eutectoid solid solution was obtained at all investigated positions by SEM-EDS analysis (Figs 18 and 19).

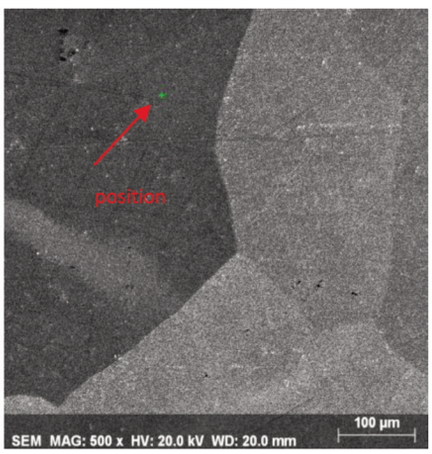

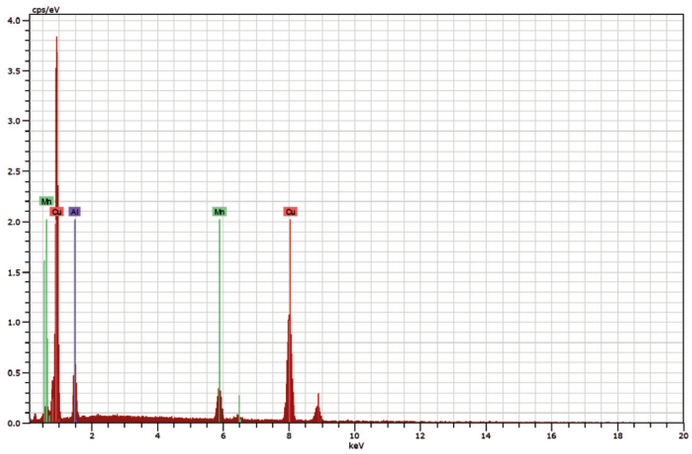

Spectrum: 4-poz 6

El	AN	Series	unn. C [wt.%]	norm. C [wt.%]	Atom. C [at.%]	Error [%]
Cu	29	K-series	80.41	81.03	70.83	2.3
Al	13	K-series	9.45	9.53	19.61	0.5
Mn	25	K-series	9.38	9.45	9.55	0.3
		Total:	99.24	100.00	100.00	

Figure 18. *EDS analysis at position 1 of sample Cu-11.4%wt. Al- 10.1%wt. Mn*

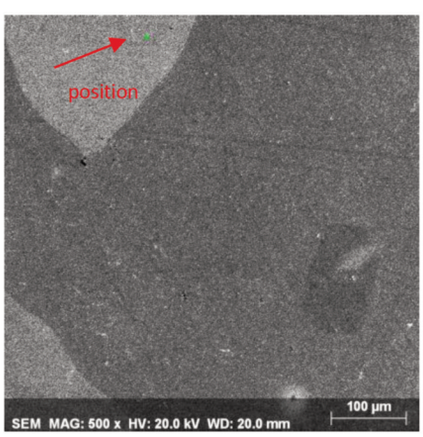

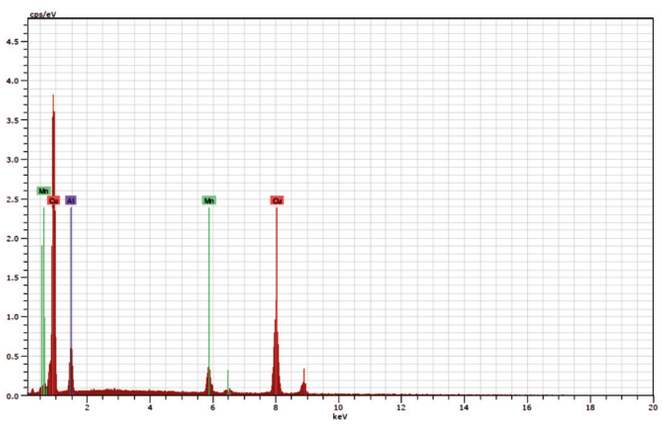

Spectrum: 4-poz 3

El	AN	Series	unn. C [wt.%]	norm. C [wt.%]	Atom. C [at.%]	Error [%]
Cu	29	K-series	82.51	81.43	71.49	2.3
Al	13	K-series	9.30	9.18	18.98	0.5
Mn	25	K-series	9.51	9.39	9.53	0.3
		Total:	101.33	100.00	100.00	

Figure 19. *EDS analysis at position 2 of sample Cu-11.4%wt. Al- 10.1%wt. Mn*

Conclusion

Four as-cast Cu-rich Cu-Al-Mn alloys with variable contents of Al and Mn were explored in presented study. Thermodynamic calculations produced equilibrium phases for each composition as well as their stability intervals, which were experimentally tested by DSC and confirmed by XRD measurements. Evaluated phase transformation temperatures through experiment procedure show reasonable agreement with theoretically predicted values. Optical microscopy, scanning electron microscopy and XRD analysis mainly confirmed thermodynamically predicted phase morphology. Cu-Al-Mn alloy with 1.2 %wt. of aluminum showed precipitation of α-Mn in Cu matrix with fcc crystal structure. Alloys with higher aluminum and manganese content show presence of α-phase and τ_3-phase, while Cu-11.4 %wt.Al-10.1 %wt.Mn alloy achieved eutectoid solid solution.

Acknowledgements

This work has been fully supported by Croatian Science Foundation under the project IP-2014-09-3405.

References

[1] C.A. Canbay et all, Acta Phys. Pol. A. 125, 5 (2014) 1163-1166.

[2] R. Dasgupta, A. K. Jain, P. Kumar, S. Hussain, A. Pandey, J. Alloy. Comp. 620 (2015) 60-66.

[3] N. Koeda, T. Omori, Y. Sutou, H. Suzuki et all, Mater. Trans. 46, 1 (2005) 118-122.

[4] J. Liu, H. Huang, J. Xie, Inter. J. Min. Met. Mat. 23, 10 (2016) 1-11.

[5] Y. Sutou, T. Omori, K. Yamauchi, N. Ono, R. Kainuma, K. Ishida, Acta Mater. 53 (2005) 4121-4133.

[6] T. Holjevac Grgurić et all, Thermodynamic Calculation of Phase Equilibria of the Cu-Al-Mn Alloys, Proceedings on Metallic and Non-metallic Materials, Zenica, (2016) 83-90.

[7] C.A. Canbay, A. Aydogdu, J. Therm. Anal. Calorim. 113, 2 (2013) 731-737.

[8] C.A. Canbay, S. Gudeloglu, Z. Kargoz Genz, Int. J. Thermophys. 36, 4 (2015) 783-794.

[9] C.A. Canbay, A. Aydogdu, Y. Aydogdu, J. Supercond. Nov. Magn. 24 (2011) 871–877.

[10] Y. Sutou, R. Kainuma, K. Ishida, Mat. Sci. Eng A 273-275 (1999) 375-379.

[11] Z. Chen, P. Chen, S. Li, Mat. Sci. Eng. A 532 (2012) 606-609.

[12] C. A. Canbay, S. Gudeloglu, Z. K. Genc, Int. J. Thermophys. 36 (2015) 783–794.

[13] D. S. Kanibolotsky, O. A. Bieloborodova, N. V. Kotova, V. V. Lisnyak, J. Therm. Anal. Calorim. 70 3 (2002) 975-983.

[14] J.L. Murray, Al-Cu (Aluminum-Copper), Phase Diagrams of Binary Copper Alloys, P.R. Subramanian, D.T. Chakrabati, D.E. Laughlin, ASM International, Materials Park, OH, 18-42 1994.

[15] V.S. Sudavtsova, N.V. Kotova, L.A. Romanova, Inorg. Mat. 45 6 (2009) 631-634.

[16] A.I. Zaitsev, N.E. Zaitseva, R.Y. Shimko, N.A. et all, J. Phys. Condens. Matter. 19 20 (2008)

[17] P.D. Desai, J. Phys. Chem. Ref. Data 16 1 (1987) 109-124.

[18] Murray, J.L., Int. Met. Rev. 30 (1985) 211-233.

[19] R. Kainuma, N. Satoh, X. J. Liu, I. Ohnuma, K. Ishida, J. Alloys Comp. 266 (1998) 191-200.

[20] McAlister, A.J., Murray, J.L., The Al-Mn (Aluminum-Manganese) System, Bull. Alloy Phase Diagrams, 8 (1987) 438-447.

[21] X.J. Liu, I. Ohnuma, R. Kainuma, K. Ishida, J. Phase Equilib. 20 1 (1999) 45-56.

[22] Landolt-Börnstein, Numerical Data and Functional Relationship in Science and

Technology, Springer Verlag, Berlin, Heidelberg, (2002) 132-169.

[23] Y. Sutou et all, Inc. J Biomed Mater Res Part B: Appl Biomater. 69B (2004) 64-69.

[24] R. Kainuma, S. Takahashi, K. Ishida, Metall. Mater. Trans. A, 27A (1996) 2187-2195.

[25] Y. Sutou, T. Omori, R. Kainuma, K. Ishida, Ductile, Mater. Sci Techn. 24, 8 (2008) 896-900.

[26] H.L. Lucas, Landolt-Börnstein, New Series IV/11A2, Springer Verlag, Berlin, Heidelberg, (2002) 79-97.

[27] J. Miettinen, Calphad 27, 1 (2003) 103-114.

[28] T. Omori, N. Koeda, Y. Sutou, R. Kainuma and K. Ishida, Materials Transactions, 48 11 (2007) 2914-2918.

[29] G. Huang, L. Liu, L. Zhang, Z. Jin, J. Min. Metall. Sect. B-Metall., 52 (2) B (2016) 177-183.

[30] A.T. Dinsdale, SGTE Data for Pure Elements, Teddington, Middlesex, UK